



HAL
open science

A new sub-nanometre error separation technique

Saint-Clair Toguem, Alain Vissiere, Charyar Mehdi-Souzani, Mohamed Damak, Nabil Anwer, Hichem Nourira

► **To cite this version:**

Saint-Clair Toguem, Alain Vissiere, Charyar Mehdi-Souzani, Mohamed Damak, Nabil Anwer, et al..
A new sub-nanometre error separation technique. EUSPEN Virtual International Conference 2020,
Jun 2020, Geneve, Switzerland. hal-02568057

HAL Id: hal-02568057

<https://hal.science/hal-02568057>

Submitted on 8 May 2020

HAL is a multi-disciplinary open access archive for the deposit and dissemination of scientific research documents, whether they are published or not. The documents may come from teaching and research institutions in France or abroad, or from public or private research centers.

L'archive ouverte pluridisciplinaire **HAL**, est destinée au dépôt et à la diffusion de documents scientifiques de niveau recherche, publiés ou non, émanant des établissements d'enseignement et de recherche français ou étrangers, des laboratoires publics ou privés.

A new sub-nanometre error separation technique

Saint-Clair T. Toguem^{1,2}, Alain Vissière¹, Charyar Mehdi-Souzani², Mohamed Damak³, Nabil Anwer²,
Hichem Nouira¹

¹ Laboratoire Commun de Métrologie, Laboratoire National de Métrologie et d'Essais (LNE-CNAM), 1 Rue Gaston Boissier, 75015 Paris, France

² LURPA, ENS Paris-Saclay, Univ. Paris-Sud, Université Paris 13, Sorbonne Paris Cité, Université Paris-Saclay, 94235 Cachan, France

³ GEOMNIA: Advanced 3D Engineering and Software Solutions, 165 Avenue de Bretagne, EuraTechnologies, 59000 Lille, France

stoquemt@ens-paris-saclay.fr

Abstract

The accuracy of roundness measurement is limited by the repeatability of measurement machines. For commercial roundness measurement machines, this limitation can be reduced by means of complex solutions to control the parameters' influence and thus limit the non-repeatable effects. The LNE-CNAM developed a cylindricity measuring machine with a particular architecture to overshoot the repeatability limitation. The working principle consists in comparing the form of the measured part with a reference form. This architecture offers the possibility of overcoming the spindle defects and consequently getting rid of the non-repeatable and random spindle error motion. The present work is about the development of an error separation technique based on the particular architecture of the new cylindricity measuring machine. In this case the separation technique consists in separating the defect of the reference form from that of the measured part. In addition, through the introduction of a one-step measurement with two sets of probes or two measurements with a set of probes, the method described here is also concerned with the minimisation of the number of operations necessary for a complete separation of errors. The effectiveness of the introduced method for a sub-nanometre error separation is proved by simulation.

Keywords – Error separation technique, spindle metrology, Fourier-based methods, harmonic distortion.

1. Introduction

The accuracy and the reliability of commercial roundness measuring machines are generally bounded by spindle imperfections. This is mainly due to their working principle which consists in comparing the form of the part to measure with a spindle motion. When it comes to cylinder measurements, there is an amplification of errors due to the combination of axes (rotation and translation). The NMI of France LNE-CNAM has developed a new high precision machine for cylinder measurements that cope with these limitations by means of original design concepts [1-3].

One important concept of the machine developed by the LNE is the DMT concept (Dissociated Metrology Technique), applied to avoid random error effects on the measurements. This concept leads to a particular working principle which consists in comparing the form of the measured artefact with a reference form (Figure 1). Hence, one can overcome the effects of spindle error motion and especially non-repeatable spindle error motion. Therefore, the challenge is only in separating the form of the artefact from that of the reference. This working principle opens new doors to the enhancement of the accuracy of roundness and cylindrical form measurements. Studies must accordingly be conducted to investigate new error separation techniques suitable for this new working principle.

A number of such error separation techniques have previously been developed [3-4]. The present study is motivated by the need for an error separation technique providing a great flexibility in terms of probes arrangement and artefact positioning. The intention is to develop an error

separation technique that suitably takes advantage of the current probes arrangement on the machine. Furthermore the developed method should also address the minimisation of the number of acquisitions.

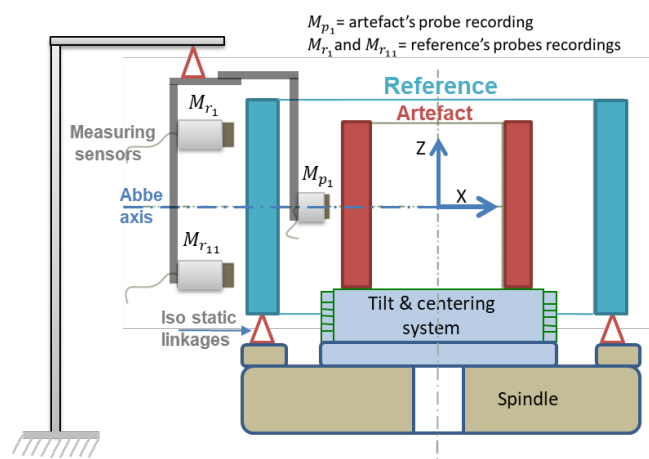


Figure 1. Partial schematic of the DMT architecture of the LNE machine

The next sections of this paper first introduce the new error separation technique theoretical development. Then an investigation into the harmonics suppression phenomenon will lead to the definition of systematic guidelines for an optimal choice of angular shifting. Finally, the effectiveness of the method will be highlighted through simulations.

2. The new error separation technique

2.1. Theoretical development

As depicted in Figure 2, the introduced method consists in performing a set of $N + 1 \geq 2$ measurements with an angular shifting of φ_i between the artefact and the reference for the measurement i . In the following, the reference is not moved during the whole process. The initial angular shifting φ_0 is set to zero.

During the measurements, probes record the reference and artefact's form but also spindle error motion (repeatable and non-repeatable), thermal drift, their own non-linearity and measurement noise from the acquisition system. The thermal drift can be considerably reduced by controlling the

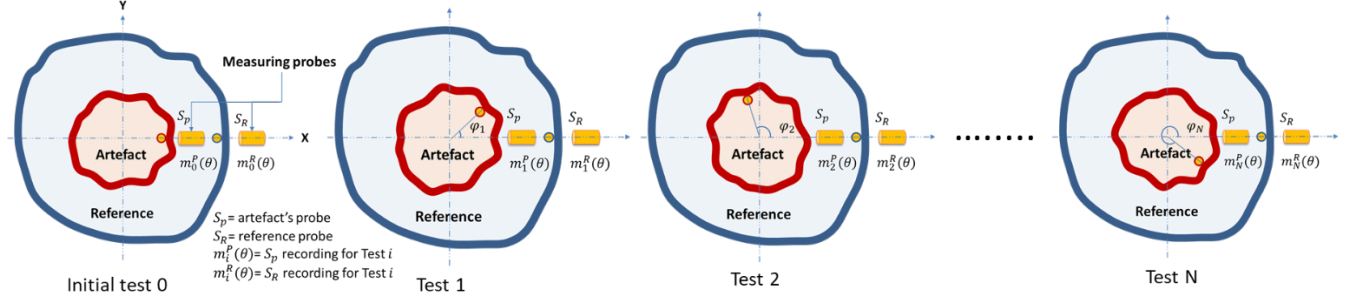


Figure 2. Schematic of the new error separation method

In the following, it is assumed that the conditions are met to neglect thermal drift, measurement noise and non-linearity errors. The remaining information in probes' recordings are repeatable and non-repeatable spindle error motion and the form of measured parts (artefact and reference). In the context of the LNE's new machine's architecture, the reference and the artefact are mounted on the same spindle. Therefore, the artefact and reference probes (respectively S_p and S_R) aligned along the same axis with the same orientation measure the same spindle error motion (figure 2). Thus, for the initial test 0, we have:

$$\begin{cases} m_0^p(\theta) = P(\theta) + Br_{X_S}(\theta) + Br_{X_{AS}}^0(\theta) \\ m_0^R(\theta) = R(\theta) + Br_{X_S}(\theta) + Br_{X_{AS}}^0(\theta) \end{cases} \quad (1)$$

Where :

$$\begin{cases} P = \text{artefact's form} \\ R = \text{reference form} \\ Br_{X_S} = \text{repeatable spindle error motion along axis X} \\ Br_{X_{AS}}^0 = \text{non repeatable spindle error motion along axis X} \end{cases}$$

For any other measurement i ($1 \leq i \leq N$), the artefact form measured by the artefact probe is φ_i phase shifted. For the reference probe, only the non-repeatable spindle error motion varies :

$$\begin{cases} m_i^p(\theta) = P(\theta - \varphi_i) + Br_{X_S}(\theta) + Br_{X_{AS}}^i(\theta) \\ m_i^R(\theta) = R(\theta) + Br_{X_S}(\theta) + Br_{X_{AS}}^i(\theta) \end{cases} \quad (2)$$

Spindle error motion (repeatable and non-repeatable) is overcome through a difference between the recordings of the artefact's probe m_i^p and the reference probe m_i^R as follows:

$$\Delta_i(\theta) = m_i^p(\theta) - m_i^R(\theta) = P(\theta) - R(\theta - \varphi_i) \quad (3)$$

An appropriate linear combination of the differences Δ_i of the $N+1$ tests, helps isolating the artefacts form. This means

temperature in the working volume but also by choosing the appropriate material for the reference. It is advantageous to choose materials with a sufficiently low expansion coefficient both for the artefact and the reference. In practice, an alternative approach is to choose for the reference, a cost-effective material with the same coefficient of expansion as the artefact so as to have the same dilatation for both the artefact and the reference in a controlled environment [3][5]. Probes' non-linearities can be significantly reduced by an appropriate calibration [3][6]. To deal with noise from the acquisition system, an efficient solution is to use a convenient setting (cutoff filters, cables type and lengths, acquisition rate) coupled with a spatial and temporal averaging of the measurements (by using capacitive probes for instance).

finding a $N+1$ tuple $(a_0, \dots, a_N) \in \mathfrak{R}^{(N+1)*}$ verifying the following equation :

$$\sum_{i=0}^N a_i = 0 \quad (4)$$

In this condition (Eq.4.), we get :

$$S(\theta) = \sum_{i=0}^N a_i \Delta_i = \sum_{i=0}^N a_i P(\theta - \varphi_i) \quad (5)$$

With $\varphi_0 = 0$.

In order to extract the artefact's form, the combined signal $S(\theta)$ is transformed from spatial domain to the harmonic domain. This can be accurately be done with a discrete Fourier transformation (DFT) since inter-harmonics represented by non-repeatable spindle errors are cancelled from the signal in Eq.3. Therefore, the DFT $\mathbf{S}(\mathbf{k})$ and $\mathbf{P}(\mathbf{k})$ of respectively $S(\theta)$ and $P(\theta)$ can be defined as follows:

$$\begin{cases} \mathbf{S}(\mathbf{k}) = \frac{1}{M} \sum_{m=0}^{M-1} S(m) e^{\frac{2j\pi m \mathbf{k}}{M}} \\ \mathbf{P}(\mathbf{k}) = \frac{1}{M} \sum_{m=0}^{M-1} P(m) e^{\frac{2j\pi m \mathbf{k}}{M}} \end{cases} \quad (6)$$

Where M is the number of collected points during one circular profile measurement (number of samples).

It therefore comes from Eq. 5 and 6 that:

$$\mathbf{S}(\mathbf{k}) = \left(\sum_{i=0}^N a_i e^{-j\mathbf{k}\varphi_i} \right) \mathbf{P}(\mathbf{k}) \quad (7)$$

If we define $\mathbf{W}(\mathbf{k}) = \left(\sum_{i=0}^N a_i e^{-j\mathbf{k}\varphi_i} \right)$, it comes that:

$$\mathbf{S}(\mathbf{k}) = \mathbf{W}(\mathbf{k}) \cdot \mathbf{P}(\mathbf{k}) \quad (8)$$

In the frequency domain, \mathbf{P} is obtained from Eq. 8 and the artefact's form P in the time domain come by the inverse discrete Fourier transformation of \mathbf{P} . Furthermore, knowing the artefact's form, the reference form R is deduced from the initial acquisition as follows :

$$R(\theta) = P(\theta) - \Delta_0(\theta) \quad (9)$$

When only two measurements are performed ($N = 1$), the method comes down to a reversal method since the artefact is moved only once. This offers the possibility to perform a complete and stable separation with only two sets of measurements. Furthermore, it opens new perspectives in reversal error separation with a high flexibility on the value of the angular shifting. For high precision designers, this means a great suppleness in probes arrangement. In practice, such reversal method can be applied either by a one-step measurement with two sets of probes or two measurements with a single set of two probes.

The complex function W can be considered as the transfer function from P to S . It determine the accuracy of the errors separation. There are some values of the frequency variable k depending on the angular position φ_i which leads to a zero transfer function. This results in the suppression of the corresponding harmonics. This problem, also encountered in classic multiprobe methods is therefore closely linked to the values of the angles φ_i chosen. Consequently, the next step is about choosing the optimal values of the angles φ_i to avoid harmonic suppression.

2.2. Choice of optimal angles

As in classic multiprobe methods, the harmonic suppression phenomenon is highly dependent on the values of the angular position φ_i . Several studies aiming at determining the optimal angular positions have been conducted in the case of classic multiprobe method. Zhang et al. [7], proposes an approach based on a non-linear optimisation problem. With minor modifications this method will be widely used in the form of complex non-linear optimisation [7-8]. However, this approach does not lead to a single optimal solution. In fact, the problem leads to several local optimums. The solution domain is therefore represented by a fractal. Nevertheless, this approach made it possible to highlight the non-optimal character of a regular angular position (e.g. 120° and 240°) [9]. Chen [10] later introduced a multi-objective matrix approach which additionally takes into account the effects of software calculation and approximation errors. More recently a direct calculation method was proposed by Baek [11]. If this new method does not take into account the effects of software-related errors, it leads to the determination of several optimal values of angular positions.

In the case of the present method, harmonic suppression occurs at frequency k_φ where the module of the transfert function W is zero (Eq. 10). In practice, depending on the accuracy of the calculator used, this phenomenon may also occur when $|W(k_\varphi)|$ is very close to zero.

$$|W(k_\varphi)| = 0 \quad (10)$$

Similarly to the classic multiprobe, the first coefficient of the $N+1$ tuple (a_0, \dots, a_N) can be set to 1 ($a_0 = 1$). This is to reduce the number of coefficients a_i to determine. Thus, Eq.10 gives:

$$\left| 1 + \sum_{i=1}^N a_i e^{-jk_\varphi \varphi_i} \right| = 0 \Leftrightarrow \begin{cases} 1 + \sum_{i=1}^N a_i \cos k_\varphi \varphi_i = 0 \\ \sum_{i=1}^N a_i \sin k_\varphi \varphi_i = 0 \end{cases} \quad (11)$$

Knowing Eq. 4, the positive solution domain of Eq.11 is in the following form:

$$\mathbb{K}_h = \bigcap_{i=1}^N \left\{ \frac{2\pi k_{\varphi_i}}{\varphi_i}, k_{\varphi_i} \in \mathbb{N}^* \right\} \quad (12)$$

For correct separation, the sampling must be performed exactly at a regular angular sampling interval $\Delta = \frac{2\pi}{M}$ so that:

$$N_{\varphi_i} = \frac{\varphi_i}{\Delta} \quad (13)$$

Therefore, \mathbb{K}_h can be reformulated in an irreducible fraction as follows:

$$\mathbb{K}_h = \bigcap_{i=1}^N \left\{ k_{\varphi_i} \cdot \frac{\left(\frac{M}{M \wedge N_{\varphi_i}} \right)}{\left(\frac{N_{\varphi_i}}{M \wedge N_{\varphi_i}} \right)} = n_{\varphi_i}, \quad k_{\varphi_i} \in \mathbb{N}^* \right\} \quad (14)$$

Where $M \wedge N_{\varphi_i} = HCF(M, N_{\varphi_i})$.

Eq. 14 predicts the harmonics suppressed during the separation. To satisfy Eq.14, n_{φ_i} as well as k_{φ_i} are integers. Therefore, any $k_\varphi \in \mathbb{K}_h$ is a multiple of $N_{\varphi_i}/(M \wedge N_{\varphi_i})$. Thus, to accurately perform the separation throughout the frequency region of interest, it is convenient to maximise $N_{\varphi_i}/(M \wedge N_{\varphi_i})$. To do this, it is advantageous to always minimise $M \wedge N_{\varphi_i}$.

For a correct error separation without harmonic suppression, the following steps can be taken to keep the minimum harmonic suppressed out of the harmonics region of interest :

From the number of samples M , the sampling rate f_r , and the consistent revolute speed $\omega = 2\pi f_r/M$, compute the angular sampling interval $\Delta = f_r/\omega$. For each measurement i , choose N_{φ_i} greater than the maximum value of interest of the harmonics. N_{φ_i} should also be chosen in order to minimise $M \wedge N_{\varphi_i}$. Compute the corresponding angle φ_i . Use simulated data to validate the suitability of the angles φ_i . Repeat the previous steps until the simulated residuals of the separation is satisfying.

3. Simulations

In order to validate the introduced method, a case study is conducted on simulated data. The simulation is performed in the case of a minimum number of measures (two measures with one angular shifting of the artefact).

The simulated artefact's form $P(\theta)$ contains harmonics with amplitudes between 8 and 10nm and a number of undulations per revolution (upr) between 5 and 35upr. For the reference form $R(\theta)$ the harmonic amplitudes vary between 1 to 4nm and a number of upr between 5 and 58upr. The amplitudes of the repeatable spindle error motion represented by the synchronous error motion $Br_{X_s}^i$ vary between 2 and 20nm with less than 21upr. For the non-repeatable or asynchronous error motion $Br_{X_{AS}}^i$, a white noise generator with a maximum amplitude of 5nm is used.

The optimal angle is calculated using the previous guidelines. The number of samples per revolution is fixed to $M = 5050000$. The sample rate f_r is set to 505 Hz. The maximum frequency of interest is 58upr. As depicted in the summarising Table 1, the obtained optimal angle is $\varphi_1 = 74^\circ 39' 43''$. N_{φ_1} is chosen as a prime number in order to form with M a set of coprime integers. This ensures a minimal value of the $HCF(M, N_{\varphi_1})$.

Table 1. Optimal angle evaluation

φ_1		74°39'43"
Parameters	$k_{maxinterest}(upr)$	58
	M	5050000
	$f_r(Hz)$	505
	$\Delta(\mu degree)$	71
	N_{φ_1}	1047341
$M \wedge N_{\varphi_1}$		1

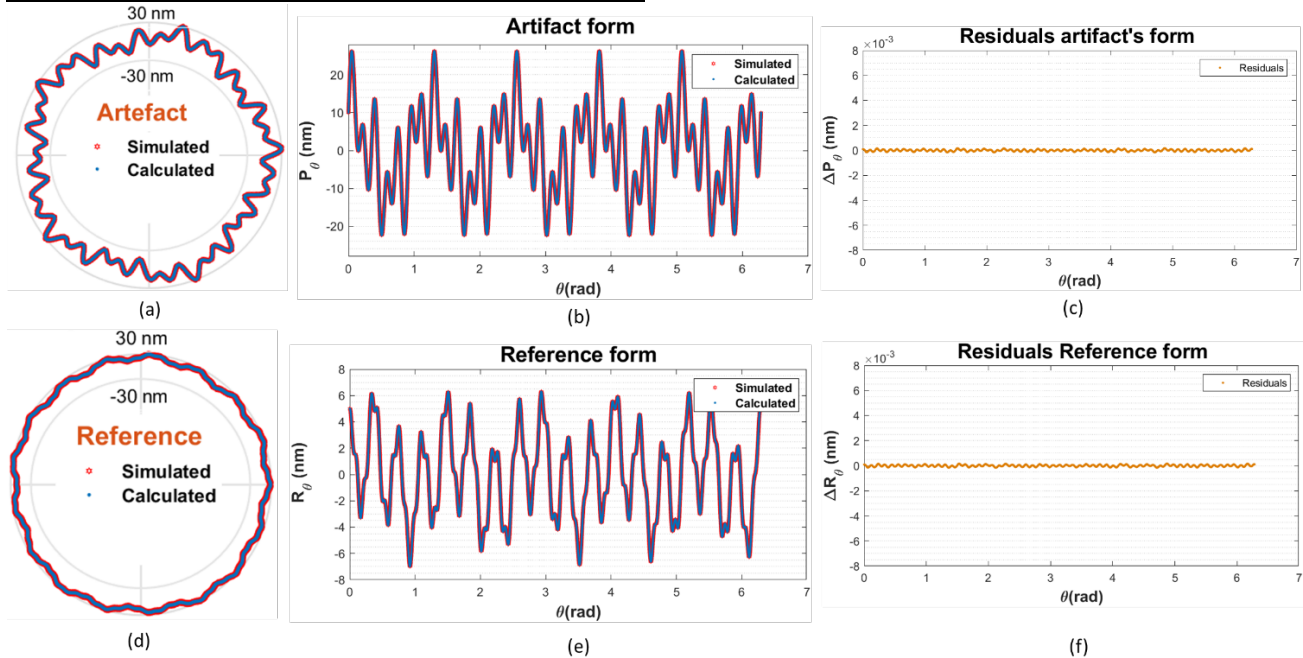


Figure 3. Simulation results: (a) & (b) artifact form; (d) & (e) reference form; (c) artifact residuals; (f) reference residuals

4. Conclusion

The purpose of the current study was to introduce a new error separation technique based on the DMT architecture of a cylindricity measuring machine. The method has been detailed in a general point of view. The new design perspectives given by the introduced method in terms of probes arrangement have been pointed out. A mathematical analysis leads to the introduction of a systematic approach for the choice of optimal shifting angles to avoid the harmonics suppression phenomenon during the separation.

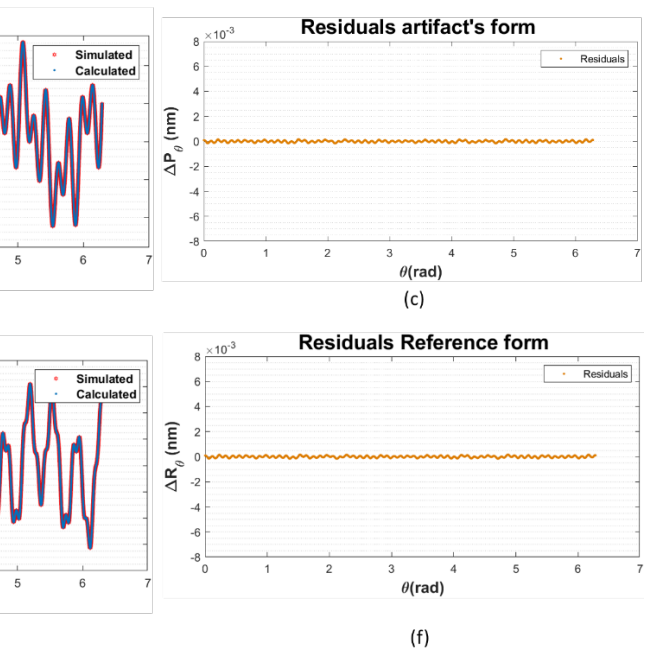
The method has been applied by simulation in the particular case of a minimal number of two measures. The results prove the effectiveness of the separation method with a sub-nanometre discrepancy less than 10^{-4} nm.

Further investigations on the robustness of the introduced method with respect to error sources (such as sensor and artefact positioning and alignment errors) through Monte Carlo simulations will lead to an uncertainty budget estimation. Future work will also focus on experimental investigations of the introduced method. This will lead to a detailed comparison with the other methods previously developed in the context of DMT architectures.

References

[1] A. Vissiere, H. Noura, M. Damak, O. Gibaru, et J.-M. David, « Concept and architecture of a new apparatus for cylindrical form measurement with a nanometric level of accuracy », *Measurement Science and Technology*, **23**, n° 9, p. 094014, sept. 2012, doi: 10.1088/0957-0233/23/9/094014.
 [2] S.-C. T. Toguem, A. Vissière, M. Damak, C. Mehdi-Souzani, N. Anwer, et H. Noura, « Design of an ultra-high-precision machine for form

The next Figure 3 shows the results of the simulation. The simulated and the recalculated artefact and reference form are presented respectively in figure 3 (a)-(b) and (d)-(e). The residuals of both the recalculated artefact and reference form are within the order of 10^{-4} nm. This discrepancy is mainly due to software approximations errors during the DFT computation. This can be ameliorated by enhancing the accuracy of the DFT operator.



measurement », *Procedia CIRP*, **84**, p. 942-947, janv. 2019, doi: 10.1016/j.procir.2019.04.262.
 [3] A. Vissière, *Mesure de cylindricité de très haute exactitude : Développement d'une nouvelle machine de référence*, PHD Thesis, Arts et Métiers ParisTech, 2013. <https://pastel.archives-ouvertes.fr/pastel-00967204>.
 [4] A. Vissiere, H. Noura, M. Damak, O. Gibaru, et J.-M. David, « A newly conceived cylinder measuring machine and methods that eliminate the spindle errors », *Measurement Science and Technology*, **23**, n° 9, p. 094015, sept. 2012, doi: 10.1088/0957-0233/23/9/094015.
 [5] A. Vissière, H. Noura, M. Damak, O. Gibaru, Implementation of capacitive probes for ultra-high precision machine for cylindricity measurement with nanometre level of accuracy, *Int. J. Precis. Eng. Manuf.* **16** (2015) 883–893, doi.org/10.1007/s12541-015-0116-z.
 [6] H. Noura, A. Vissiere, M. Damak, et J.-M. David, « Investigation of the influence of the main error sources on the capacitive displacement measurements with cylindrical artefacts », *Precision Engineering*, **37**, n° 3, p. 721-737, juill. 2013, doi: 10.1016/j.precisioneng.2013.02.005.
 [7] G. X. Zhang et K. Wang, « Four-Point Method of Roundness and Spindle Error Measurements », p. 4.
 [8] S. Cappa, D. Reynaerts, et F. Al-Bender, « A sub-nanometre spindle error motion separation technique », *Precision Engineering*, **38**, n° 3, p. 458-471, juill. 2014.
 [9] Huang JianJian, Ma Ping, et Li DuanNeng, « The effect of positioning error and noise on the accuracy for spindle rotation error measurement with three-point method », in *The 2nd International Conference on Information Science and Engineering*, Hangzhou, China, 2010, p. 1596-1599.
 [10] Y. Chen, X. Zhao, W. Gao, G. Hu, S. Zhang, et D. Zhang, « A novel multi-probe method for separating spindle radial error from artifact roundness error », *Int J Adv Manuf Technol*, **93**, n° 1-4, p. 623-634, oct. 2017.
 [11] S.-W. Baek, M.-G. Kim, D.-H. Lee, et N.-G. Cho, « Multi-probe system design for measuring the roundness and rotation error motion of a spindle using an error separation technique », *Proceedings of the Institution of Mechanical Engineers, B: Journal of Engineering Manufacture*, **233**, n° 5, p. 1547-1560, avr. 2019.